Minerals Engineering 69 (2014) 205–213

Contents lists available at ScienceDirect

Minerals Engineering

journal homepage: www.elsevier.com/locate/mineng

A CFD-kinetic model for the flotation rate constant, Part II: Model validation

M. Karimi *, G. Akdogan, S.M. Bradshaw

Department of Process Engineering, Stellenbosch University, Private Bag X1 Matieland 7602, Stellenbosch, South Africa

ARTICLE INFO

Article history:
Received 19 September 2013
Revised 12 April 2014
Accepted 11 May 2014
Available online 13 June 2014

Keywords:
Computational Fluid Dynamics
Flotation modelling
Flotation rate constant
Validation

ABSTRACT

A Computational Fluid Dynamics (CFD) model was validated against published experimental data for the prediction of the flotation rate constant. An Eulerian–Eulerian framework was applied for modelling the multiphase flow inside a standard laboratory scale Rushton turbine flotation tank. The dispersed k–ε turbulence model simulated the turbulent effects inside the tank, while the collision, attachment and stability efficiencies were calculated using the local values of hydrodynamic parameters. Volume-weighted average flotation rate constants were simulated for chalcopyrite and galena and compared against published experimental data for the same physical setup. The results showed that both qualitatively and quantitatively the developed CFD-kinetic model can predict the flotation rate constants with an acceptable level of accuracy. Moreover, the validations of rate constants for the flotation of chalcopyrite and galena under various contact angles, agitation rates and gas flow rates confirmed the predictive capability of this numerical approach for further flotation modelling.

1. Introduction

The separation of valuable minerals from gangue in a flotation tank is achieved through the successful occurrence of three sub-processes. These sub-processes start with collision between the hydrophobic solid particles and the air bubbles. After collision, the intervening liquid film between the solid particle and the air bubble thins out and eventually ruptures, leading to the attachment phenomenon. The solid–liquid–gas interface moves on the surface of the air bubble to establish a stable bubble–particle aggregate. This rises to the froth phase where it can be collected in the launder (Gaudin, 1932; Schuhmann, 1942; Schulze, 1983; King, 2001).

The schematic illustration of the flotation sub-processes is given in Fig. 1, where the light coloured circle represents the air bubble, the thick dashed line corresponds to the liquid film encompassing the air bubble and the small dark circle displays the solid particle.

Derjaguin and Dukhin (1993) and Dukhin et al. (1995) suggested that the collection efficiency of solid particles is the product of three probability functions, quantifying the collision, attachment, and detachment efficiencies. Therefore, the general form of the flotation kinetic model can be derived as Eq. (1):

$$\frac{dN_p}{dt} = kN_p = -Z_{pb} \times E_c \times E_a \times E_s \tag{1}$$

where N_p is the number of solid particles, k is the flotation rate constant, Z_{pb} is the number of bubble–particle collisions and the efficiencies of the collision, attachment and stability are represented by E_c, E_a and E_s, respectively. Eq. (1) describes the kinetic aspect of the flotation separation process, while the sub-processes are involved using three efficiency functions.

Previous research has focussed on developing formulations for the flotation sub-processes in such a way that the effects of hydrodynamic parameters and operational conditions are reflected by the probabilities of the bubble–particle collision, attachment and stability. Throughout the various studies in this field (Schubert and Bischofberger, 1978; Gorain et al., 1995a,b, 1996, 1997; Bloom and Heindel, 1999, 2003; Heindel and Bloom, 1999; Dai et al., 1999, 2000) the influence of hydrodynamic factors on the flotation responses (i.e., flotation recovery and rate constant) has been emphasized. One of the important contributions in the field of flotation modelling was developed at the Ian Wark research institute in Australia (Pyke et al., 2003; Duan et al., 2003). The fundamental flotation model due to Pyke correlates the flotation rate constant with three major features of the separation process including the mechanical aspects of the cell, the hydrodynamic

* Corresponding author. Tel.: +27 21 808 3860, mobile: +27 71 745 7038; fax: +27 21 808 2059.
E-mail addresses: karimimp@gmail.com (M. Karimi), gakdogan@sun.ac.za (G. Akdogan), smb@sun.ac.za (S.M. Bradshaw).

http://dx.doi.org/10.1016/j.mineng.2014.05.014
0892-6875/

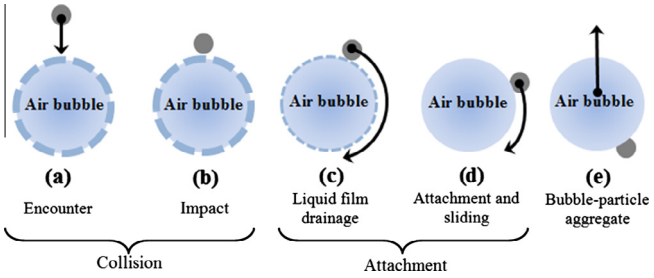

Fig. 1. Schematic representation of the flotation sub-processes.

characteristics of the turbulent flow, and finally the sub-processes occurring between solid particles and air bubbles. The capability of the model was examined for the predictions of quartz, chalcopyrite and galena flotation rate constants (Newell, 2006; Pyke, 2004). Acceptable agreement with the experimental measurements was achieved, when modifications (i.e., averaging or calibration) were applied for the hydrodynamically important factors such as the bubble velocity and the turbulent dissipation rate. Beside Pyke's work, the common method to determine the hydrodynamic factors of the flotation tank has been the application of a single value for these parameters. For instance, the energy dissipation rate has been obtained as the ratio of power input over the mass of fluid within the tank (Newell and Grano, 2007). However, the fluctuating nature of the hydrodynamic terms might cause errors in the prediction of flotation performance. Schubert (2008), for example, pointed out that the maximum energy dissipation rate adjacent to the rotational system is 200 times stronger than the average energy dissipation rate at the bulk flow region. Therefore, it is apparent that using a method in which the fluctuation of local values of flow variables are integrated into the model is likely to result in more accurate predictions than lumped parameter models.

Computational Fluid Dynamics (CFD) offers an alternative to the use of spatially-averaged values for the hydrodynamic factors in the flotation modelling. CFD can provide detailed information on the transient and fluctuating characteristics of the hydrodynamic factors within the vessel. Application of CFD allows us to remedy the weakness of the empirically-based models for the flotation process (i.e., the application of invariant hydrodynamically important flow parameters). In other words, by incorporating the turbulent fluctuating flow variables into the micro processes of the flotation the differences between the model predictions and reality has been reduced. As a result, application of numerical approaches for the flotation separation modelling can improve the state of art for the prediction of flotation performance.

The numerical challenges encountered for single-phase and multiphase modelling of agitated tanks have been comprehensively addressed in the literature (Bakker and Van den Akker, 1994; Lane et al., 2000, 2005; Ranade et al., 2002; Murthy et al., 2007; Joshi et al., 2011). It has been reported that an inexpensive CFD model for stirred tanks should apply the Multiple Reference Frames (MRF) method to mimic the impeller rotation. In addition, for gas–liquid modelling, the turbulent effects on the dispersed phase should be accounted for with an appropriate formulation for the drag force. Although the details for the CFD modelling of a fully turbulent multiphase flow inside stirred tanks are available in open literature, there exist a limited number of papers dealing with the numerical modelling of flotation tanks. This can be explained by the fact that the sub-processes occurring inside the flotation tank multiply the complexities experienced for the application of CFD. Koh et al. (2000) computed the number of bubble–particle collisions for two types of flotation tanks using Abrahamson equation (Abrahamson, 1975). In 2003, (Koh and Schwarz, 2003) applied an Eulerian–Eulerian multiphase approach along with the standard k–ε turbulence model to simulate the collision and attachment rate in a Denver-type flotation machine assuming that the attachment probability was unity. Their CFD model was able to predict the dissipation rate of turbulence, the volume fraction of each phase and the bubble–particle collision pattern. The computed collection rate constant showed higher values than the typical industrial flotation rate constant and that was attributed to the differences in the transport times between the laboratory and the industrial scale tanks. In a follow up study in 2006 (Koh and Schwarz, 2006), an extra transport equation was added to the previous Eulerian–Eulerian framework to determine the removal rate of the bubble–particle aggregates. Source and sink terms were also introduced for the additional equation to address the attachment and detachment phenomena. Based on the ratio of free particles to the total particles in the cell, they computed the flotation rate constant. A similar methodology was applied in 2007 for a self-aerated tank (Koh and Schwarz, 2007) and in 2009 for Microcel column and Jameson flotation cell (Koh and Schwarz, 2009). Validation was also performed in 2010 with the experimental flotation recoveries of ballotini glass beads (Koh and Smith, 2010). A year later, the influence of stirring speed and the induction time on the flotation performance was investigated using the same CFD model (Koh and Smith, 2011).

Any CFD-based method for modelling of flotation cells should offer improved prediction of responses compared with empirically-based methods, and when compared with other CFD methods, should be computationally more economical. Furthermore, the developed CFD methodology should be independent of the mineral types and capable of predicting the flotation behaviour of different minerals with various hydrophobicities. The first part of this study (Karimi et al., 2014) focused on the development of the CFD-kinetic model. The fundamental flotation model due to Pyke for the flotation rate constant (Pyke, 2004) was used as the basis for the incorporation of the transient CFD data for the computation of micro- and macro-scale flotation parameters. Experimental data for quartz particles, adopted from Newell (2006) and Pyke (2004), with $d_{100} < 106$ μm floating under different angular velocities of impeller, contact angles, and gas flow rates were used to investigate the capability of the new CFD-based approach. The numerical predictions were compared to the measurements and the analytical calculations using spatially-averaged values for the hydrodynamic parameter in Pyke's equation. The results showed that for quartz particles the CFD-kinetic model was able to produce either compatible or improved predictions of the flotation rate constants, when it was compared with the experiments and the analytical computations. The implemented model differed from that of Koh and Schwarz by predicting the flotation rate constant directly without the necessity for solving an extra partial differential equation for the number concentration of free particles. This procedure not only eliminates the need for defining the source and sink terms to account for the flotation sub-processes but also decreases the overall computational effort. In the earlier paper (Karimi et al., 2014), the model was applied only to the prediction of quartz flotation rate constants, which yielded acceptable agreement with experimental data.

In this paper, we investigate the capability of the CFD-kinetic model for the prediction of flotation rate constants of two industrially-relevant minerals, chalcopyrite and galena, floating under different agitation rates, gas flow rates, and particle surface hydrophobicities. In order to validate the CFD results the experimental measurements of Pyke (2004) for chalcopyrite and galena have been used. In his work different hydrophobicity levels (i.e. contact angles) were achieved through using various dosages of different collector types. For instance, 50 and 100 g/t of sodium ethyl xanthate resulted in contact angles of 56° and 67° for chalcopyrite, whereas different concentrations of Di-iso-butyl-phosphinate